ANNUAL REVIEWS

Annual Review of Physical Chemistry

First-Principles Simulations of Biological Molecules Subjected to Ionizing Radiation

Karwan Ali Omar,[1,2] Karim Hasnaoui,[3,4] and Aurélien de la Lande[1]

[1]Institut de Chimie Physique, CNRS UMR 8000, Université Paris-Saclay, 91405 Orsay, France; email: aurelien.de-la-lande@universite-paris-saclay.fr

[2]Department of Chemistry, College of Education, University of Sulaimani, 41005 Kurdistan, Iraq

[3]High Performance Computing User Support Team, Institut du Développement et des Ressources en Informatique Scientifique (IDRIS), 91403 Orsay, France

[4]Maison de la Simulation, CNRS, Commissariat à l'Energie Atomique et aux Énergies Alternatives (CEA), Université Paris-Saclay, 91191 Gif-sur-Yvette, France

Annu. Rev. Phys. Chem. 2021. 72:445–65

The *Annual Review of Physical Chemistry* is online at physchem.annualreviews.org

https://doi.org/10.1146/annurev-physchem-101419-013639

Keywords

radiation chemistry, first-principles simulations, real-time time-dependent density functional theory, RT-TDDFT, charge migration, radical chemistry

Abstract

Ionizing rays cause damage to genomes, proteins, and signaling pathways that normally regulate cell activity, with harmful consequences such as accelerated aging, tumors, and cancers but also with beneficial effects in the context of radiotherapies. While the great pace of research in the twentieth century led to the identification of the molecular mechanisms for chemical lesions on the building blocks of biomacromolecules, the last two decades have brought renewed questions, for example, regarding the formation of clustered damage or the rich chemistry involving the secondary electrons produced by radiolysis. Radiation chemistry is now meeting attosecond science, providing extraordinary opportunities to unravel the very first stages of biological matter radiolysis. This review provides an overview of the recent progress made in this direction, focusing mainly on the atto- to femto- to picosecond timescales. We review promising applications of time-dependent density functional theory in this context.

1. INTRODUCTION

The discovery that high-energy radiation has major physiological effects dates back to the early days of radioactivity at the beginning of the twentieth century. In her PhD thesis (1), Marie Curie reviewed the observations of Walkhoff, Giesel, Becquerel, and P. Curie that skin exposure to radium causes red blotches or even blisters in the case of longer exposure, noting in the meantime the first attempts made at the Hospital Saint-Louis in Paris to use radium-emitted rays to cure skin diseases. She also mentioned the deleterious effects of the rays produced by radium on plant leaves, which turned them yellow and caused them to become friable. She further reported Giesel's observations that the development of microbial populations is slowed upon exposure to radium, although moderately. More than a century later, we know that the radiation emitted by radioactive elements (α or β^- particles) or X-rays is ionizing radiation (IoR). IoR interacts so strongly with the electron cloud of molecules composing the cell that it induces their ionization. Energy deposition triggers a cascade of physicochemical events that leads to the formation of chemical lesions on essential-for-life biomacromolecules such as DNA, proteins, and lipids. The term IoR actually refers to a wider family of particles that encompasses both high-energy photons (extreme ultraviolet rays, X-rays, and γ-rays) and charged particles (e.g., atomic nuclei, electrons, positrons, and muons) in the kilo-electronvolt to mega-electronvolt kinetic energy range (2).

IoR has either natural (rocks, seas, sun, or cosmos) or anthropogenic (medicine, nuclear plant wastes, nuclear plant disasters, or nuclear weapons testing) origins. The exposure of the human body to IoR is deleterious, as the induced radiation damage causes metabolic dysfunction and accelerated aging as well as contributes to the appearance of cancerous tumors (3). DNA has long been considered to be the main biomacromolecule that accounts for the physiological consequences of irradiation (3). This makes sense because DNA is at the core of the genetic information storage system. Without minimizing the importance of DNA, however, evidence has accumulated that irradiation of other cellular machinery, for example, mitochondria in eukaryotic cells (4–6), ion channels (7), and cellular structures such as lipid layers (8), also contributes to cellular responses to irradiation.

Astronauts placed beyond the Earth's magnetosphere are subjected to intense solar and cosmic rays (composed of a majority of 1 MeV protons but also of heavier elements). This represents a major obstacle to future space exploration, e.g., to moon colonization or the exploration of Mars by humans (9).

Besides these deleterious effects, we should also consider the strategies devised by physicians to harvest the devastating power of IoR in radiotherapeutic treatments aimed at killing cancer cells. At the dawn of the twenty-first century, particle therapies relying on either protons or heavier atomic nuclei (e.g., C^{6+}), eventually coupled with the use of radiosensitizers (10), are updated radiotherapies that should permit more controlled dose delivery, hence alleviating the risks of irradiating the surrounding healthy tissues (11, 12). One can logically expect that detailed knowledge of damage formation at the molecular level will help to unravel the molecular basis of such particle therapies and contribute to their development.

A current main topic of research remains the formation of clustered damage along the particle tracks (13–15). Clustered damage is associated with base excision and DNA–DNA or DNA–histone cross-links as well as single- and double-stranded breaks. When such damage is formed in dense clusters, DNA repair by the cell becomes difficult if not impossible (16, 17). These clusters can also modify the epigenetic regulation of gene expression if key chemical functionalizations on histones are altered (18, 19). Their molecular mechanisms of formation largely await discovery.

Pioneering experiments by Sanche and coworkers (20–22) combining irradiation by external electron sources with well-controlled kinetic energies (1.8 to 20 eV) and chemical analyses of the degradation products have revealed the ability of low-energy electrons (LEEs) to induce damage

in DNA and peptides. The underlying mechanisms start with electron attachment within shape- or core-excited Feshbach resonances (21), followed by energy redistribution into vibrational modes, eventually leading to bond breaking. While the studies in the Sanche laboratory were carried out on solid-state samples, the first evidence of the reactivity of the presolvated electron in the liquid phase was reported comparatively recently (23, 24). For example, Mostafavi and coworkers (23) reported different reactivity for the near-free electron compared with that for the solvated electron with uracil monophosphate, showing that only the former induces bond breaking between the base and the ribose. These data probe the production, diffusion, and reactivity of LEEs in natural biological structures. This is another front that should stimulate active research in the near future.

We wish to mention two other research areas in which IoR is thought to be a central player. One of these areas is interstellar chemistry. Several ongoing projects aim to clarify the role of IoR in the formation of prebiotic molecules on comets or icy grains (25) and also, presumably, in the atmospheres of Jupiter's and Saturn's natural satellites (26). The other research area is biomolecular 3D imaging by X-ray diffraction techniques. X-ray photon beams induce radiation damage during data recording (27). Research is ongoing to determine, for example, the location and chemical composition of damage within DNA–protein complexes (28). The recent advent of extreme free-electron lasers that drastically reduce the duration of sample exposure alleviates this risk, but no definitive solution seems to have yet been reached by the community of crystallographers (27).

We finally stress the extraordinary opportunities that are emerging from the development of attosecond or ultrafast spectroscopies (29–31). While traditional time-resolved pulsed radiolysis using beams of charged particles has been essentially limited to the picosecond regime (see, e.g., 32), leaving a thick veil on the physical chemistry taking place at earlier times, attosecond science is clearly changing the situation. For example, the measurement of one of the earliest chemical events in water radiolysis ($H_2O^{\bullet+} + H_2O \rightarrow HO^{\bullet} + H_3O^+$) could be recently time-resolved for the first time by using tunable femtosecond soft X-ray pulses from an X-ray free-electron laser (29). Other studies (e.g., 33) have led to proposed new reaction channels, leading to the formation of dicationic water clusters by intermolecular Coulombic decay (ICD). These first studies doubtlessly pave the way toward exciting discoveries in the coming years.

Theory and computer modeling have been mobilized for many years to assist in the interpretation of experimental data, and excellent reviews have been published (34–38). The great variety of methodologies developed in the field cannot be summarized here. We instead adopt a complementary perspective and paint a state-of-play of the first-principles approaches dedicated to molecular simulations of the radiolysis of biological matter. Most importantly, we attempt to pinpoint the current methodological roadblocks that, from our point of view, need to be overcome. We have made the arbitrary choice to focus on first-principles methodologies that capture the dynamics of the phenomena at play in the formation of radiation damage. We have decided to focus on the first stages of the radiolysis of biological matter, covering energy deposition to ultrafast chemistry, on which important progress has been made in recent years. In addition, we occasionally borrow examples of applications from related fields such as materials science.

2. THE HALLMARKS OF RADIATION CHEMISTRY

Following IUPAC (International Union of Pure and Applied Chemistry), we make a clear distinction between radiation chemistry and photochemistry. Admittedly, both deal with chemical reactivity involving electronic excited states and, in biology, can lead to severe damage to biomacromolecules. However, the initial excitation is very different and consequently triggers different physicochemical responses. In photochemistry one usually deals with long-duration light pulses having well-defined energies of at most a few electronvolts. Irradiation vibrationally

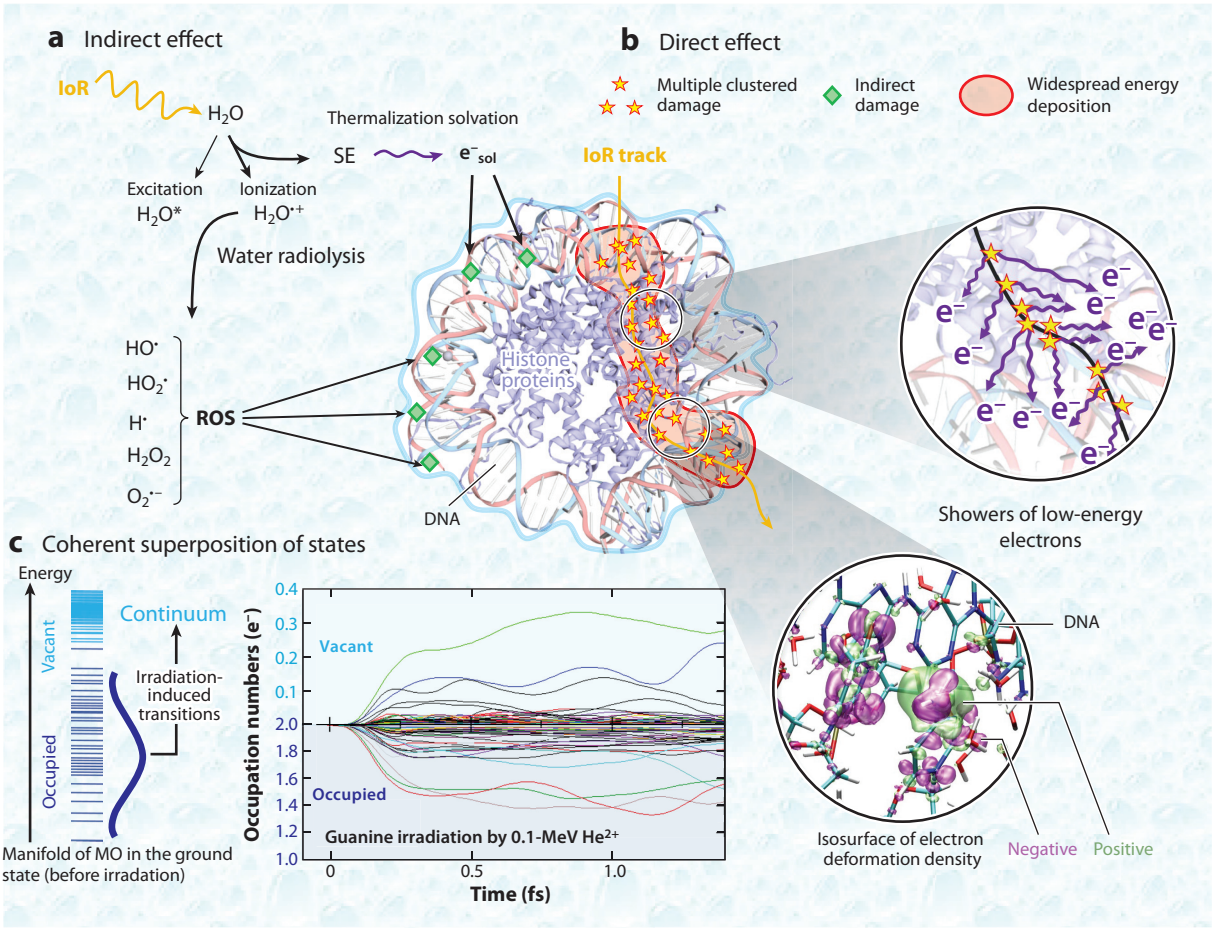

Figure 1

The hallmarks of IoR irradiation, illustrated for the case of a nucleosome—a 12-nm-wide assembly of DNA wrapped around a core of histone proteins—irradiated by a charged particle (α, β, μ, or others). (*a*) Water radiolysis produces ROS and SEs that attack biomacromolecules after diffusion (*green diamonds*, indirect effect). (*b*) Direct irradiation of the nucleosome induces widespread energy deposition (*red zone*) with copious emission of low-energy electrons and ultimately formation of dense multiple clustered damage. (*c*) An attosecond collision of a 0.1-MeV α particle with a DNA base produces a superposition of quantum states; this is reflected by many initially occupied MOs that become partially depopulated (*lower part* of graph), while many initially unoccupied MOs become partially populated (*upper part* of graph). Abbreviations: IoR, ionizing radiation; MO, molecular orbital; ROS, reactive oxygen species; SE, solvated electron; sol, solvated. Figure adapted with permission from Reference 39.

or electronically excites molecules selectively, populating in general one given excited state. In **Figure 1** we illustrate a case of radiation chemistry, a large biological architecture subjected to irradiation by a charged projectile. The central image depicts a nucleosome, an assembly of a 146-base-pair double-stranded DNA molecule wrapped around a core made of 8 histone proteins. Charged particles interact with matter by Coulomb scattering. Projectiles of kinetic energy in the kilo-electronvolt to mega-electronvolt energy range mainly interact with electrons along their propagation tracks, impacting primarily valence electrons. The amount of energy deposited can be huge, increasing to several tens of electronvolts per molecule (39), and energy deposition is widespread along the projectile track. As the duration of interaction is very short, on the

subfemtosecond timescale, collisions produce quantum superpositions involving a large number of electronic excited states (**Figure 1*c***). IoR produces, by definition, a huge number of low-energy electrons that further irradiate the surrounding matter. Via the Compton effect, γ-rays interact with matter, producing showers of high-energy secondary electrons that ionize the surrounding matter. X-rays interact via the photoelectric effect, targeting core-shell electrons. X-ray ionization opens specific evolution channels involving, for instance, Auger decays (40) and ICD (41).

Damage triggered by IoR customarily has been classified as stemming from indirect or direct effects (compare **Figure 1*a*** and **1*b***). The indirect effect refers to damage initiated by water radiolysis ($H_2O \rightarrow H_2O^{\bullet+} + 1e^-$), which produces reactive oxygen species that diffuse before attacking a wide variety of chemical functions on biomacromolecules (42). Direct damage is caused by energy deposition in the biomacromolecules themselves (43). For the sake of completeness, we also mention the quasi-direct effect proposed by Sevilla and coworkers in the 1990s (44) to describe ultrafast charge transfer between DNA, and by extension other biomacromolecules, with $H_2O^{\bullet+}$ produced by irradiation in the first hydration shell of biomacromolecules (e.g., $DNA + H_2O^{\bullet+} \rightarrow DNA^{\bullet+} + H_2O$).

The responses of matter subjected to IoR are truly multiscale (**Figure 2**) and have been customarily classified according to the kind of processes involved in the successive temporal sequences. The definition and the borders between successive stages are of course arbitrary, but this classification helps to set up concepts. The physical stage refers to the deposition of energy, including electronic excitations, ionizations, and other purely electronic processes [ICD (41), charge migration (45), Auger decay, and energy relaxation and dissipation]. One can determine the end of the physical stage when the nuclear response starts to be significant, thereby entering the physicochemical stage. Within a few picoseconds, a very complex nonadiabatic dynamics coupling electronic to nuclear motion can lead to fragmentations, molecular explosions, or the production of a myriad of chemically harsh radicals. The attachment of low-energy electrons to biomacromolecules also takes place during the physicochemical stage. Once the dust has started to settle, chemical

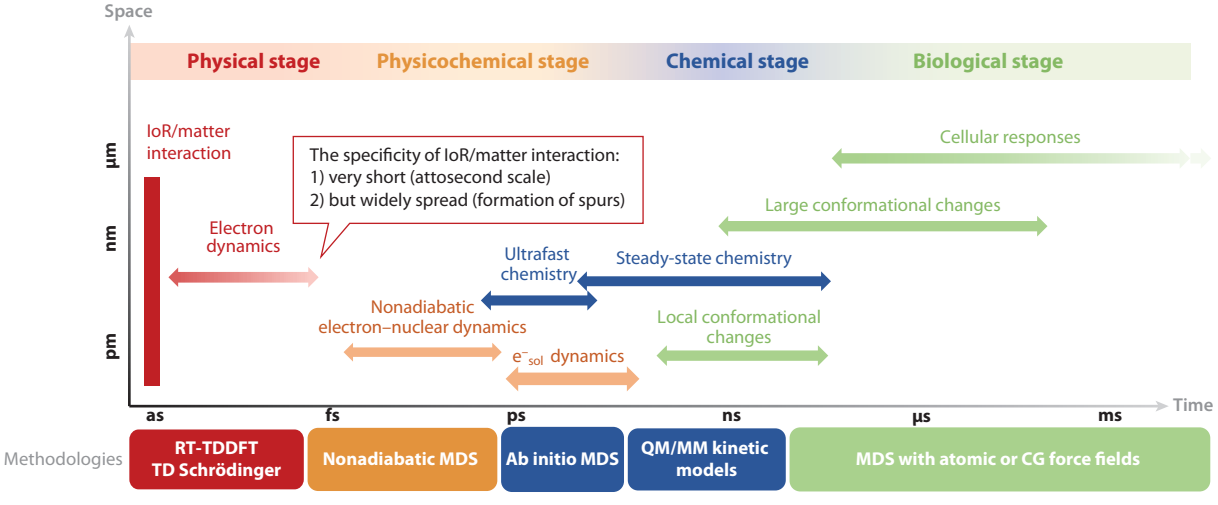

Figure 2

(*Top*) The interaction of IoR with biological matter induces multiscale responses in time and space. (*Bottom*) A list indicating some of the major methodologies found in the literature to address these different scales. Abbreviations: CG, coarse grained; IoR, ionizing radiation; MDS, molecular dynamics simulation; MM, molecular mechanics; QM, quantum mechanics; RT-TDDFT, real-time time-dependent density functional theory; TD, time dependent.

reactivity taking place under thermodynamic equilibrium governs the formation of damage to biomacromolecules. The biological stage finally refers to the consequences for the structure and dynamics of damaged biomacromolecules. It also covers the metabolic responses of the cell, which include at least the detection and reparation of DNA damage by the cellular machinery and some epigenetic responses as well as adaptation of the energy generation machinery (e.g., mitochondria).

This description of the multiscale responses of biomacromolecules irradiated by IoR guides us in the next section. Common methods found in the literature to simulate the physical and physicochemical stages are Monte Carlo track structure (MCTS) algorithms (46, 47). MCTS algorithms rely on sets of parameterized elementary cross sections (excitation/ionization, electron scattering, electron attachment, and others) to stochastically simulate the succession of physical and physicochemical events in the medium. Although valuable to deal with homogeneous media, these approaches face insurmountable hurdles with the staggering number of events to parametrize for biological molecules, especially in terms of chemical reactions. Some chemical reactions may also turn out to be impossible to identify and to parametrize in advance. Furthermore, MCTS algorithms rely on important hypotheses (e.g., transferability of the parameters and static description) that are hardly justified for highly heterogeneous biological systems. First-principles methodologies thus represent valuable alternatives, as discussed in the next section.

3. FIRST-PRINCIPLES SIMULATIONS OF THE PHYSICAL STAGE

3.1. Electron Dynamics Simulations

Simulating the physical stage is challenging, as the objective is to capture strong electronic excitations in large molecular systems, with emission of electrons into the continuum. The so-called good old quantum chemistry toolbox that deals with electrons bound to molecules is not directly usable. Wave functions for electrons in the continuum are delocalized and exhibit oscillatory behavior that is not easily captured by standard basis sets. The choice of a particular methodology is generally guided by (*a*) the nature of the ionizing radiation that determines the kind of initial excitation to be modeled as well as the subsequently available evolution channels, and (*b*) the trade-off between accuracy and computational cost and the level of accuracy one is willing to sacrifice. Some researchers working in the field of attosecond science proposed the combination of Gaussian basis functions to describe bound electrons with B-splines to describe electrons in the continuum (48). Excellent agreement was obtained with such schemes to reproduce experimental cross sections of Ne photoionization, and application to medium-sized molecules is on the way. The treatment of resonances is another difficult task to address. To this end, Krylov and coworkers (49) have extended the equation-of-motion coupled cluster method to the use of complex absorbing potentials with promising applications. A dedicated scheme using configuration interaction has been developed to capture Fano resonances (50). Progress has also been made in the context of density functional resonance theory (51).

For the treatment of large and realistic molecular models, simulations based on time-dependent DFT (TDDFT) (52) represent a workhorse. To simulate the physical stage one can simulate step-by-step the response of the electronic cloud subjected to a perturbation by discretizing time into small time steps, typically of a few attoseconds, and by propagating TDDFT equations (53, 54). Within the Kohn-Sham (KS) framework, the basic equation-of-motion reads as

$$i\frac{\partial \rho\,(r,t)}{\partial t} = [H\,(r,t)\,,\,\rho\,(r,t)] \qquad 1.$$

$$H(r,t) = T_{\mathrm{s}}\,[\rho(r,t)] + v_{\mathrm{ee}}[\,\rho(r,t)] + \quad + v_{\mathrm{Z}} + v_{\mathrm{IoR}}, \qquad 2.$$

where T_s is the kinetic energy functional of the KS noninteracting electron gas; v_Z and v_{ee} are the potentials created by the atomic nuclei and by the electron cloud, respectively; v_{XC} is the exchange-correlation potential; and v_{IoR} is the potential created by the IoR.

For photon irradiation, a classical dipole approximation is often assumed by which the electronic system interacts with the electric field component of the electromagnetic light [$\mathbf{F}_{IoR}$ (bold characters indicate vectors)] through its molecular dipole, i.e., $v_{IoR} = \mathbf{F}_{IoR} \bullet$ d. The mathematical form of $\mathbf{F}_{IoR}$ can be shaped to mimic specific light sources, such as continuous light or a Gaussian electric pulse. A more realistic description of photon–electron interaction has been presented recently by an approach bridging DFT and quantum electrodynamics (55). This promising approach treats the photon and the electrons as being on equal footing at the quantum level of description.

Charged particles interact with matter via the Coulomb interaction. For heavy projectiles (H^+, He^{2+}, or other heavier ions), a classical representation can be adopted, and v_{IoR} is conveniently calculated from a relativistic Liénard-Wiechert formula (56). For lighter projectiles, notably electrons, the situation is more delicate, as one can hardly ignore the quantum nature of the projectile. We are not aware of methodologies described in the literature to simulate such irradiation by real-time TDDFT (RT-TDDFT). Rizzi et al. (57) attempted to simulate electron injection into small water chains, comparing two methodologies: one using an electron pulse and another a steady stream of electrons. They highlighted the difficulties of controlling injection conditions, but they paved the way for more realistic simulations in the future. Some help might also come from conceptual developments within the exact factorization formalism (58) or from multicomponent DFT (59).

Having set up the KS Hamiltonian, accurate and stable algorithms are available to propagate TDDFT equations (60, 61). Computer codes for RT-TDDFT have flourished in the last two decades, some with impressive performance (62–64). We have developed an RT-TDDFT implementation within the context of auxiliary DFT (ADFT) (65). ADFT uses variational density fitting (66) to substitute in a controlled manner the electron-repulsion potential and the exchange–correlation (XC) potential computed directly from KS orbitals for quantities evaluated from fitted densities developed over monocentric basis functions. An advantage of the local basis set ansatz used in the software package deMon2k (67) for DFT calculations is that hybrid or range-separated XC functionals that incorporate a fraction of exact exchange remain tractable even for large molecular systems (68, 69). A further advantage of ADFT comes from the possibility of carrying out repetitive on-the-fly analyses of the time-dependent electronic structures without introducing supplementary computational costs (70). **Figure 3** illustrates the computational performance of our current CPU (central processing unit)-based implementation. The four most computationally demanding tasks are highlighted, among which matrix exponential evaluations are the most demanding and require optimized libraries such as ScaLAPACK (71) to remain efficient. Note also the low computational cost and remarkable scaling of KS potential evaluations that is permitted by ADFT. To go larger and to tackle the molecular complexity of biological systems, we have developed a hybrid scheme coupling RT-TD-ADFT to a polarizable Amber ff02 molecular mechanics force field (72, 73). Our implementation includes retardation in the electric field propagation that mediates the polarization of the two regions (56).

Electron dynamics (ED) simulations can be carried out at a fixed nuclear position (so-called purely RT-TDDFT simulations), but nuclear motion can be straightforwardly coupled via the Ehrenfest molecular dynamics (MD) approach (74, 75). In this case, atomic nuclei are assumed to move according to Newton's law ($\mathbf{F}_A = m_A.a_A$, where $\mathbf{F}$ is the force acting on nucleus A, m is its mass, and a its acceleration) and the forces acting on the nuclei are calculated directly from the average potential energy provided by RT-TDDFT, namely $\mathbf{F}_A = \partial E[\rho(t)]/\partial R_A$. Ehrenfest MD

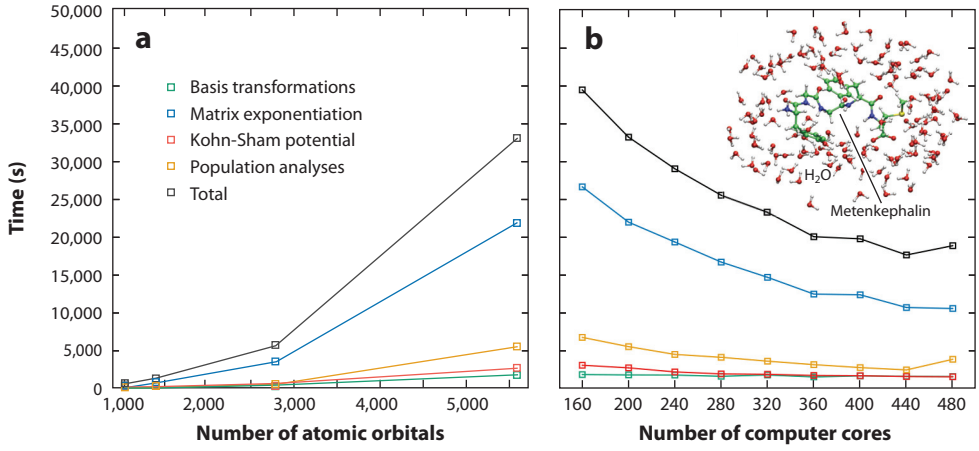

Figure 3

Computational performance of real-time time-dependent auxiliary density functional theory (RT-TD-ADFT) in deMon2k using the example of a solvated metenkephalin (see inset in panel *b*). The simulation consists of a 200-as electron dynamics simulation (a 1-as time step with a predictor–corrector scheme) that extracts atomic charges at every time step. (*a*) This graph shows computational cost as a function of the thickness of the solvation layer (from 0 to 6 Å) and reflected by the number of atomic orbitals. (*b*) This graph indicates scaling performance with the number of computer cores for the 6-Å solvation layer.

opens the way to the simulation of both the physical and physicochemical stages. Examples of applications are given in Section 4.

3.2. Electronic Stopping Power Calculations with Real-Time Time-Dependent Density Functional Theory

Stopping power (SP) is a property characterizing energy deposition by a projectile in matter as a function of the kinetic energy of the projectile. It is defined as the derivative of the total potential energy with respect to the projectile displacement (76). As a consequence of the mass difference between atomic nuclei and electrons, and that both interact with charged projectiles, the total SP can be decomposed to a good approximation into a nuclear component and an electronic component. Both exhibit a concave shape but have different maximum positions. Nuclear SP dominates over electronic SP at low kinetic energy (<0.01 MeV/nuc), while electronic SP is predominant between 0.01 and a few hundreds of MeV/nuc. Electronic SP for many projectile types and materials has been measured for decades and collected in data banks available online (77, 78). These SP values are sometimes complemented by semiempirical data obtained by the application of analytical models such as Bethe's theory (79). The electronic SP is thus an ideal target property to assess the reliability of RT-TDDFT to simulate energy deposition by charged projectiles. Overall, the results obtained by various groups so far are encouraging (76, 80–82). First, calculated electronic SP curves have been found to be of similar shape and amplitude as the experimental curves for projectiles in the kilo-electronvolt to mega-electronvolt kinetic energy range. However, a conclusion emerging from various studies (81, 83) is a marked sensitivity of SP with the basis set. The pressure put on the basis set quality depends on the energy region in which one is interested. Around the SP maximum, a good description of valence electrons is mandatory, while at high projectile energies, contributions from core excitations must be properly considered (83).

SP calculations seem to be weakly sensitive to XC effects. The simplest local density approximation (LDA) already provides similar results to generalized gradient approximation (GGA) or hybrid GGA XC functionals (53). This can be understood by the fact that energy deposition is driven primarily by Coulomb interactions and only marginally by XC effects. Even though encouraging, a more in-depth understanding of this finding is needed. In fact, most LDA or GGA functionals are known to inadequately position Rydberg or charge-transfer states and to notably underestimate ionization potentials (84). Thus, even though the densities of states generated by different functionals produce similar energy depositions, the nature of the populated excited states might be drastically different. If so, the subsequent dynamics might be XC functional–dependent, eventually producing irrelevant charge-migration mechanisms. We also note that previous simulations have been carried out under the adiabatic approximation. This consists of ignoring the explicit time dependence of the XC potential $v_{XC}[\,\rho(r,t)] \rightarrow v_{XC}[\rho(r)]$. As irradiation can be accompanied by abrupt variations of the electron density with compressions or dilations (85, 86), XC functionals incorporating memory and dissipation effects might be mandatory (87). Nonetheless, the first applications of RT-TDDFT SP calculations are encouraging for applications of the methodology to biological models.

3.3. Electron Dynamics Simulations in Biomolecules

Water is probably worth considering as a prime biological molecule. Privett et al. (88) investigated the one-electron transfer from water clusters containing from one to six molecules, to 0.1 MeV H^+. They employed a simplest-level-electron nuclear dynamics method and found qualitative agreement with available experimental cross sections for the smallest clusters. Reeves & Kanai (89) reported purely RT-TDDFT-based SP calculations on systems comprised of 162 water molecules with periodic boundary conditions to mimic bulk water. They found the formation of the water cation (H_2O^+), with excitations primarily involving oxygen lone pairs.

The advantage of DFT-based approaches is the lower computational cost that permits the investigation of large molecular systems. Yost & Kanai (90) reported SP calculations in DNA for helium and hydrogen nuclei. The simulations were carried out on 10 base pairs of DNA (CGCGCTTAAG sequence) in the gas phase, encompassing 684 atoms and 2,220 electrons. They compared the electronic SP for collision trajectories perpendicular to the double-stranded DNA molecule to a perturbative treatment based on the Born approximation. Encouraging agreement was found between the two approaches. The authors analyzed hole formation, highlighting the contributions of high-lying occupied KS molecular orbitals to the ionization process. Interestingly, they further showed that hole production did not correlate directly with energy deposition, as generally thought. Instead maximum hole production was obtained for projectile energies lower than the Bragg peak. The origin of this difference is yet to be fully clarified.

We investigated the ionization mechanism triggered by H^+, He^{2+}, and C^{6+} ions traversing a solvated double-stranded DNA molecule by means of a hybrid RT-TD-ADFT/molecular mechanics (MM) approach (7 base pairs and 99 solvation water molecules, for a total of 742 atoms and 3,170 electrons, were described at the DFT level; see **Figure 4*a***) (91). The projectile successively struck seven molecular moieties. We revealed an ebb-and-flow ionization mechanism. As the incoming projectile is positively charged, it strongly polarizes the electron cloud when approaching a molecule, dragging the density to it (**Figure 4*b***). Immediately after collision, the electrons flow back, and a fraction of the electron density is emitted. The slower the projectile, the larger the amplitude of flow and backflow of the density (91). To what extent this so-called ebb-and-flow ionization mechanism influences energy deposition and ionization probabilities remains to be clarified, but this is another example of a process accessible only by ED simulations.

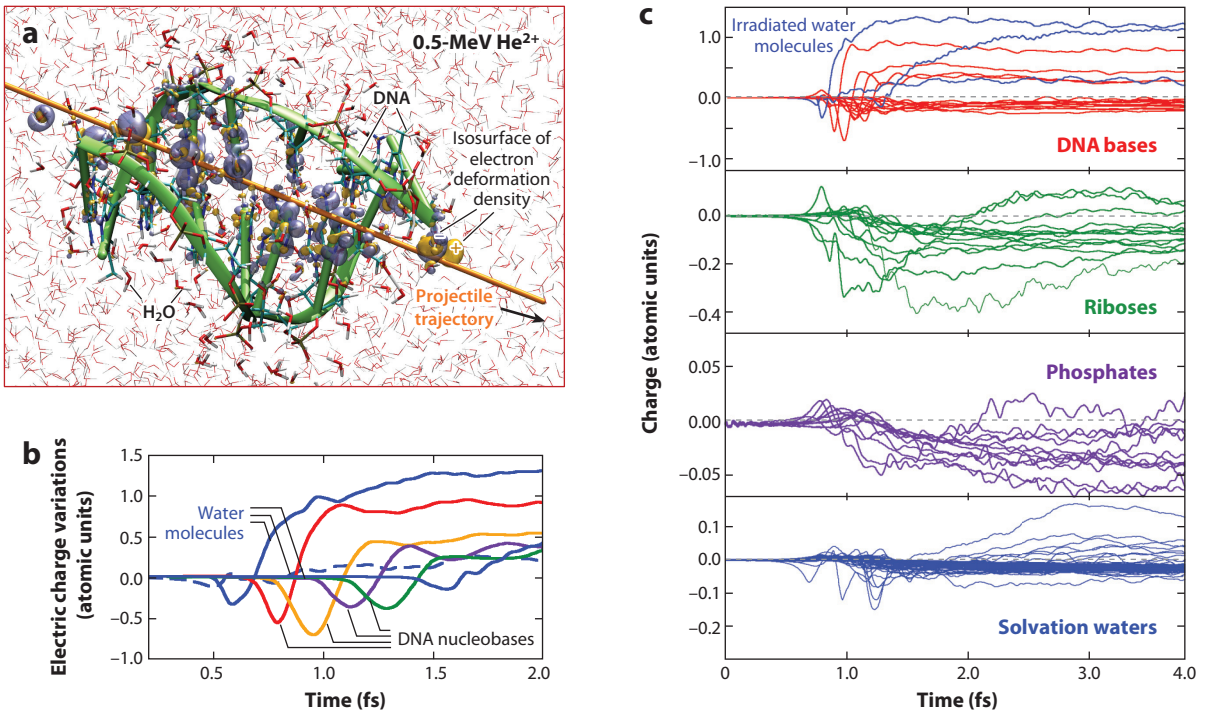

Figure 4

Irradiation of a solvated double-stranded DNA molecule by a 0.5-MeV He^{2+} ion. (*a*) Illustration showing the density just after irradiation in violet (positive isosurfaces of electron deformation density) and yellow (negative isosurfaces). The DNA double strand is shown in green. Water molecules are shown in red (oxygen atoms) and white (hydrogen atoms) licorice representation. The orange line is the projectile trajectory. (*b*) Graph showing charge variations of three water molecules (*blue lines*) and four DNA nucleobases (*red*, *orange*, *violet*, and *green lines*) struck by helium nuclei of different kinetic energies. Just before collision, the fragment accumulates electron density (its charge decreases) before releasing and becoming partially ionized. (*c*) Graph indicating charge fluctuations of all molecular fragments as a function of time. Figure adapted from Reference 91.

We found that ionization takes place in less than a few hundreds of attoseconds, independently of the projectile charge, but depending, as expected, on the projectile speed. We further investigated subsequent charge migrations, showing that holes created on the DNA base delocalize over the riboses in a few femtoseconds (**Figure 4*c***). However, similar to the conclusion of Kanai and coworkers (90), we found that holes do not migrate far away from the sites of formation. Last but not least, we identified the sites of localization of the secondary electrons. They sit on surrounding sugar-base moieties and also on the solvation layer. These findings could be helpful to understand the subsequent reactivity of low-energy electrons (see Section 4). Note that the two studies discussed here employed GGA functionals that are known to be plagued by self-interaction error. This probably affects charge migration mechanisms and needs to be investigated thoroughly.

The interplay between charge migration and nuclear motion during the very earliest stage of irradiation is still an open question. On the one hand, charge migration between the amine group and the side chain of ionized tryptophan or phenylalanine was shown to be rather insensitive to nuclear motion (31, 92, 93). By comparing RT-TDDFT simulations with Ehrenfest MD simulations, the researchers showed that during the first femtoseconds, nuclear motion had no noticeable effect on the frequencies characterizing charge migration. On the other hand, charge migration in a prototypical artificial light-harvesting system was shown to be strongly coupled to nuclear

vibrations (94). Furthermore, Vacher et al. (95) showed, using the direct dynamics variational multiconfigurational Gaussian method, that electronic decoherence already causes damping of charge migration within a few femtoseconds. In another study of charge migration within ionized polyene and glycine based on the realization of Ehrenfest MD, Polyak et al. (96) showed that dephasing was a major source of decoherence in the first femtoseconds. These apparent contradictions tend to suggest that nuclear motion and electronic decoherence are strongly system dependent. The couplings between the different vibration modes likely contribute to gate energy flows and, hence, the response of nuclear wave packets to changes in electron states. The extent to which electronic decoherence impacts the kinds of charge migration in radiation chemistry problems needs to be investigated.

3.4. Challenges for Modeling the Physical Stage

In this subsection, we discuss two classes of challenges for the first-principles modeling of radiation chemistry problems that call for methodological developments.

The first challenge is caused by other unpleasant consequences of the lack of electronic decoherence. We illustrate three of them in **Figure 5**, considering very simple systems. In **Figure 5*a***, an irradiation event has a 10% probability of ionizing a water molecule. A mean-field approach such as RT-TDDFT produces an electronic wave packet integrating to 0.1 e^-, not a wave packet integrating to 1 e^- with 10% probability. This is problematic, as a 0.1 e^- wave packet does not have the ionizing properties of a full electron, and if attached to a molecule the wave packet would only marginally reduce it. In **Figure 5*b***, the emitted wave packet is equally scattered over three directions, and then in three further directions. The irradiative properties of scattered electrons somehow become diluted. The examples shown in **Figure 5*a*,*b*** illustrate the failure of standard RT-TDDFT simulations to deal with the subsequent evolution of secondary electrons produced by irradiation. **Figure 5*c*** illustrates another well-known problem of Ehrenfest MD. It shows the radio-induced dissociation of a water molecule provided by Ehrenfest MD. Electronic decoherence is the missing piece of the puzzle needed to recover a phenomenological picture. Many schemes have been proposed, from simple patches to sophisticated algorithms (97, 98); they might need adaptation to simulation of the large molecular systems shown, for instance, in **Figure 4*a***. Recently, Wang and coworkers (99) proposed a method to enforce decoherence using information from the adiabatic state populations and applied it to the radiolysis of a small molecule.

The second challenge is related to the interpretation and visualization of data produced by simulation algorithms. Radiation chemists are used to employing terms such as single and double ionizations, excitation transfer, amount of deposited energy, kinetic energy of secondary electrons, and radicals. To what extent do the outcomes of RT-TDDFT ED and Ehrenfest MD match this phenomenological description? In the past, theoretical frameworks such as conceptual DFT (100) or topological analyses (101) were developed by quantum chemists to establish mathematical connections between the outcomes of stationary electronic structure calculations and chemical concepts (chemical bonding, electronegativity, hardness, aromaticity, and others). A similar effort should probably be made now in the context of nonstationary electron densities to extract comprehensive insights allowing the interpretation of experimental data.

In this direction, we have extended topological analyses to the realm of attosecond ED (39, 102), considering both the electron density and the time-dependent electron localization function (TD-ELF) (103). As an illustration, **Figure 6** shows a water molecule struck by a 10-keV α particle. TD-ELF topological analyses reveal how the projectile is dressed by a wave packet containing 0.8 e^-. When applied to larger systems, these analyses reveal a lot of valuable information on the evolution of the Lewis structure (**Figure 6*b***) (39). Much remains to be done, however, to apply and further develop interpretative tools for ED simulations.

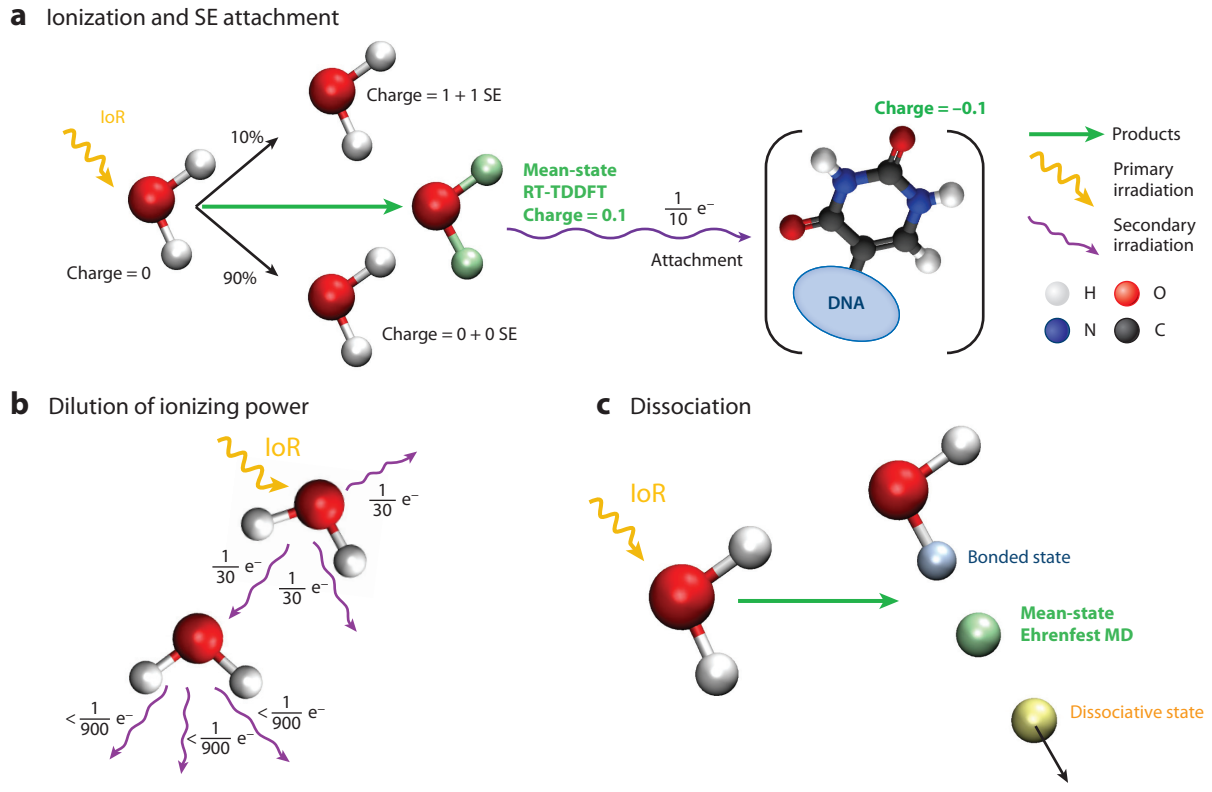

Figure 5

Simple cases to illustrate artifacts caused by a lack of electronic decoherence in pure RT-TDDFT and Ehrenfest MD. (*a*) A collision with a 10% probability of ionization produces a secondary electron wave packet holding 0.1 e^-. Attachment to a DNA base leads to a species with a charge of only −0.1, not −1. (*b*) A collision with a 10% probability of ionization produces three negligible wave packets, each having a weak ionizing property. (*c*) If ionization causes a water molecule to dissociate with 50% probability, the Ehrenfest MD trajectory is the fictitious mean bonded and dissociated molecule. Abbreviations: IoR, ionizing radiation; MD, molecular dynamics; RT-TDDFT, real-time time-dependent density functional theory; SE, solvated electron.

4. THE DYNAMICS AND REACTIVITY OF LOW-ENERGY ELECTRONS

Since the discovery that low-energy electrons can induce DNA strand breaks, computer modeling has been used to understand the underlying mechanisms governing the diffusion and reactivity of such electrons. The optical properties of the solvated electron were characterized in the 1960s in radiolysis studies, and the first attempts to investigate the hydrated electron with numerical simulations date back to the 1980s (104). Investigations of deexcitation pathways and temperature-dependent optical properties have been investigated by computer simulations (105).

In 2014, Jungwirth, Hamm, and coworkers (106) used transient terahertz spectroscopy to investigate the collapse of a free-electron wave function on the femtosecond timescale. The researchers performed ground-state simulations to investigate the associated timescales. It takes a few hundred femtoseconds for the wave function to collapse and 3 ps to form a solvation cage.

Many studies have addressed the reactivity of LEEs with the building blocks of life, in particular small DNA models. The energetics of LEE-induced strand breaks (107–109), base loss (110), and deprotonation have been reported by static approaches relying, for instance, on DFT. Various

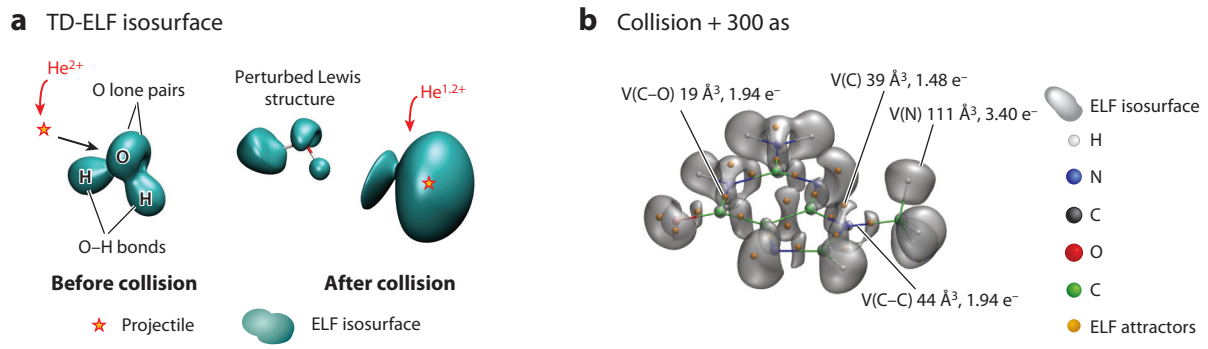

Figure 6

(*a*) Illustration showing time-dependent electron localization function (TD-ELF) isosurface (0.8) before and after the collision of a water molecule with a 10-keV He^{2+}. (*b*) Illustration showing TD-ELF topological analysis of guanine 300 as after collision. The analysis reveals the Lewis patterns, in particular the splitting of the central C–C bond. A few selected basins are shown with their volumes and electronic populations. The orange beads represent the attractors of the topological basins. Figure adapted with permission from Reference 39.

excellent recent reviews have been devoted to this topic (35, 111), to which we refer interested readers for more details.

Dynamic approaches have appeared in the last decade. Kumar et al. (111), as well as Smyth & Kohanoff (112), have investigated electron attachment from water to nucleobases by means of ground-state Born-Oppenheimer MD (BOMD) simulations. Depending on the nucleobase considered, this process was shown to take place within the range of 15 fs to a few tens of femtoseconds. Dissociative electron attachment in gas phase or environmental nucleobases was further investigated by means of BOMD and selected vibrational excitations. McAllister et al. (113) revealed the protective role of water molecules around the thymine nucleobase by increasing the barriers to N–H bond breaking. They also investigated phosphate–sugar bond breaking in nucleotides (35). In another study (114), the protective role of amino-acid residues against the bond breaking of the reduced thymine nucleobase was shown with first-principles simulations.

5. ULTRAFAST CHEMICAL REACTIVITY

Finally, we review a few examples dealing with the ultrafast chemical reactivity taking place out of thermodynamic equilibrium during the physicochemical stage. The reactivity of $H_2O^{\bullet+}$ has been the subject of insightful studies. $H_2O^{\bullet+}$ gives a proton to a surrounding water molecule ($H_2O^{\bullet+} + H_2O \rightarrow HO^{\bullet} + H_3O^+$), presumably in a few tens to a few hundreds of femtoseconds. Recently Loh et al. (29) reported three characteristic times (46 ± 10 fs, 0.18 ± 0.02 ps, and 14.2 ± 0.4 ps) that they assigned to the proton-transfer reaction, to the vibrational cooling of the hot hydroxyl radical, and to geminal recombination, respectively. Nonadiabatic MD simulations combining Hartree-Fock (using Koopmans' theorem to access excited states) with an MM force field to simulate the water environment led to a characteristic time of 60 fs for the proton transfer, which matches the experimental 46 fs reasonably well. In previous simulations carried out with DFT, Marsalek et al. (115) showed that, in the ground state, the hole is delocalized over three water molecules [i.e., $(H_2O)_3^{\bullet+}$ is a preferable notation to $H_2O^{\bullet+}$]. The amount of exact exchange introduced in the XC functional to compensate for self-interaction error is a crucial parameter that controls the degree of hole delocalization. They found that proton transfer is gated by a preliminary charge relocalization on a single water molecule that takes place in approximately 30 fs.

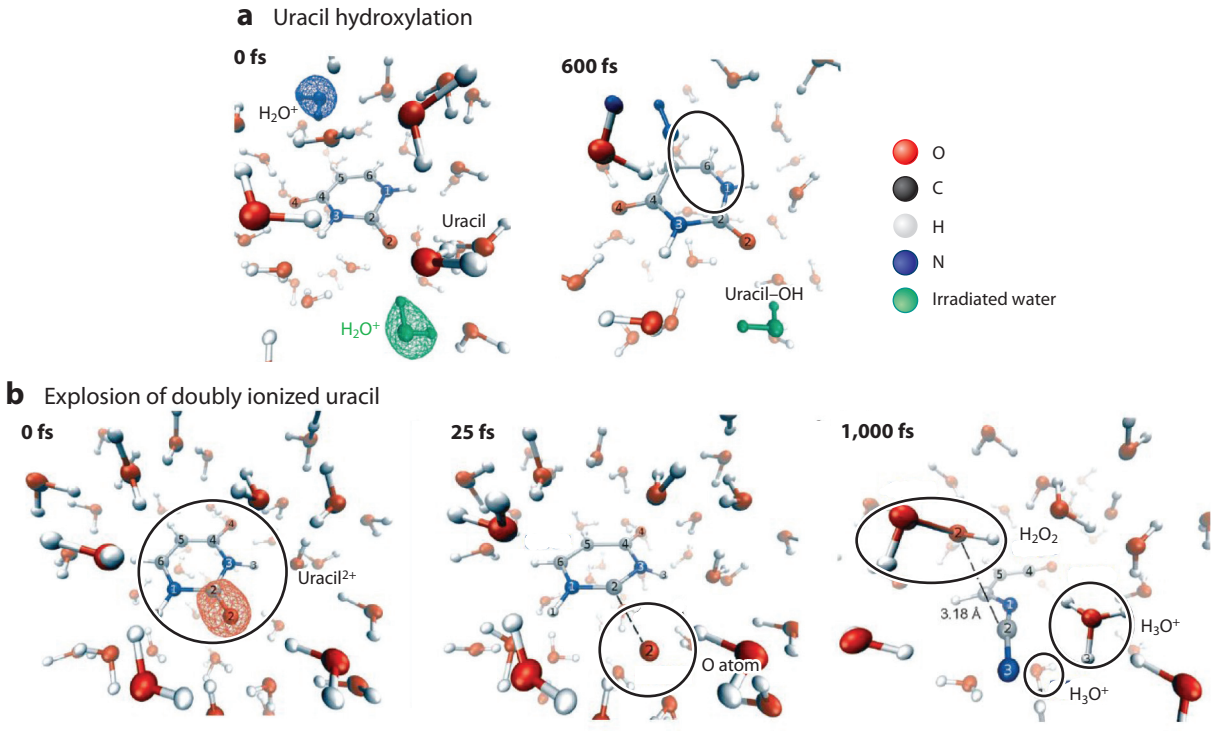

Figure 7

Illustration showing the hydroxylation of solvated uracil by H_2O^+ formed (*a*) in its solvation shell and (*b*) by Coulomb explosion after double ionization. Figure adapted with permission from Reference 117.

This is a remarkable example of a so-called attosecond chemical reaction, i.e., a chemical reaction driven by electronic motion. More investigation might be needed to compare the reactivities of the radical cation of water in the ground state versus the excited state, as well as the reactivity of biomacromolecules in bulk or in the hydration shell. In the latter situation, $H_2O^{\bullet+}$ can act as an oxidant before acting as an acid. This was proven, for example, in experimental and computational studies of pulsed radiolysis of acid solutions (116). Moreover, López-Tarifa et al. (117) discovered that when $H_2O^{\bullet+}$ is formed in the vicinity of a uracil nucleobase in water, it leads to hydroxylation of the base following an original reaction mechanism that does not involve the hydroxyl radical. This reaction takes place within 600 fs (**Figure 7**).

In a series of papers, Tavernelli and coworkers (117–121) explored the consequences of double ionizations of biorelevant molecules (water, riboses, and uracil). Double ionization is not a probable event upon proton or α-particle irradiation. It is comparatively much more probable with irradiation by heavier ions such as C^{6+} (91). In any case, if it occurs, double ionization can lead to dramatic consequences for the structural integrity of ionized molecules. Indeed, the number of negative charges held by electrons is generally not sufficient to compensate for the repulsive interactions among atomic nuclei, and a so-called Coulomb explosion can occur. An example is provided in **Figure 7*b*** for the case of uracil.

6. CONCLUSION AND PERSPECTIVES

This review is intended to portray the state of the art of first-principles simulations dedicated to the first stages of biological matter radiolysis. After having discussed some of the currently

open questions regarding the formation of radiation damage by direct effects and low-energy electrons, as well as the new opportunities brought by the advent of attosecond science, we have highlighted some recently proposed methodologies dedicated to the modeling of the physical and physicochemical stages. Most applications have dealt with small gas-phase molecules or small solvated molecules, far from the complex biological structures shown in **Figure 1**. Nevertheless, applications of RT-TDDFT to much larger systems comprised of almost 1,000 atoms at the DFT level are now accessible with various software programs, attesting to progress in the field and opening exciting perspectives for more realistic simulations.

We have drawn attention to some aspects that from our point of view are still unsatisfactorily treated. The issue of electronic decoherence is certainly a major one, as it limits the horizon of applicability of RT-TDDFT beyond the very first femtoseconds after irradiation. Another one is the need to further develop interpretative tools to analyze simulation outcomes and to extract insights that can be understood within the well-established vocabulary of radiation chemistry.

We have focused on the shortest stages of irradiation, but it is clearly necessary to bridge the gap to longer timescales. Integrative multiscale methods should be developed in the future. Although the road to reach fully realistic modeling of biological matter radiolysis is still a long and winding one, we hope we have convinced the reader that it is a thrilling research field with uncountable opportunities for young researchers.

SUMMARY POINTS

1. We have summarized the hallmarks of irradiation by ionizing radiation and have described the multiscale responses of biological molecules subjected to ionizing radiation (IoR). Current open questions are related to the complicated molecular mechanisms of clustered damage formation in DNA, proteins, or DNA–protein complexes and also the diffusion and reactivity of secondary electrons in natural biological structures. We have stressed the opportunities offered by attosecond spectroscopies to help unravel the earliest stages of radiolysis that, up to now, remained inaccessible to standard pulsed radiolysis techniques.
2. We have shown that real-time time-dependent density functional theory (RT-TDDFT) is emerging as a promising approach to simulating energy deposition by charged particles in both materials and realistic DNA models. Already, insights into the mechanisms of hole formation, subsequent charge migrations, and localization of secondary electrons can be obtained. We also have stressed some points that deserve more in-depth analyses and benchmarks.
3. We have reviewed the simulations carried out by various research groups to address the difficulties of modeling dissociative electron attachment by first-principles molecular dynamics (MD) approaches. In addition, we have covered results from other groups suggesting that the nucleobase environment strongly impacts the energy landscape of the dissociation channels.
4. We have shown that Ehrenfest MD simulations have great potential to reveal unexpected chemical reactivity taking place on the subpicosecond timescale after irradiation. Thus, while most studies have addressed small biomacromolecules in water, they pave the way for applications to more complex biological structures.

FUTURE ISSUES

1. Computational efficiency needs to be dramatically pushed forward to embrace the complexity of IoR damage, notably clustered damages. Using a range from a few thousand to ten thousand atoms seems to be a good objective. This is a challenging but probably reachable target for TDDFT-based approaches within the next few years.
2. The types of ionizing particles in RT-TDDFT should be extended to include low-energy electrons, positrons, and muons but also γ-rays, X-rays, and other electron–photon coupled channels (e.g., Auger emissions).
3. The outcomes of RT-TDDFT simulations against experimental data from attosecond spectroscopies need more validation on both small and large systems. The reliability of adiabatic and nonadiabatic exchange-correlation (XC) functionals for radiation chemistry problems needs to be fully clarified, as well as the issues arising from self-interaction error on charge migrations.
4. Conceptual tools to characterize secondary electrons produced in RT-TDDFT simulations need to be invented. For example, we need tools to evaluate their kinetic energies and their angular scattering and also to investigate the diffusion of low-energy electrons.
5. Electronic decoherence needs to be incorporated for large molecular systems.
6. Applications to larger and more realistic models of biomacromolecules should be envisioned step-by-step.

DISCLOSURE STATEMENT

The authors are not aware of any affiliations, memberships, funding, or financial holdings that might be perceived as affecting the objectivity of this review.

ACKNOWLEDGMENTS

We kindly thank Xiaojing Wu, Xiaodong Zhao, Angela Parise, and Aurelio Alvarez-Ibarra for their contributions to results reviewed in this article, as well as our collaborators for many enlightening discussions. Financial support was provided by Centre National de la Recherche Scientifique (CNRS) (Project Emergence@INC 2018) and the French Agence Nationale de la Recherche (Project RUBI; grant number ANR-19-CE29–0011–01). We are grateful to Grand Équipement National de Calcul Intensif (GENCI; project number A0060706913) and to Compute Canada for providing us with generous computational resources.

LITERATURE CITED

1. Skłodowska Curie M. 1904. *Recherches sur les Substances Radioactives*. Paris: Gauthier-Villars
2. Hatano Y, Katsumura Y, Mozumder A. 2010. Introduction. In *Charged Particle and Photon Interactions with Matter*, pp. 1–7. Boca Raton, FL: CRC Press
3. Dizdaroglu M, Jaruga P. 2012. Mechanisms of free radical-induced damage to DNA. *Free Radic. Res.* 46(4):382–419
4. Yamamori T, Yasui H, Yamazumi M, Wada Y, Nakamura Y, et al. 2012. Ionizing radiation induces mitochondrial reactive oxygen species production accompanied by upregulation of mitochondrial electron transport chain function and mitochondrial content under control of the cell cycle checkpoint. *Free Radic. Biol. Med.* 53(2):260–70

5. Yoshida T, Goto S, Kawakatsu M, Urata Y, Li T. 2012. Mitochondrial dysfunction, a probable cause of persistent oxidative stress after exposure to ionizing radiation. *Free Radic. Res.* 46(2):147–53
6. Szumiel I. 2015. Ionizing radiation-induced oxidative stress, epigenetic changes and genomic instability: the pivotal role of mitochondria. *Int. J. Radiat. Biol.* 91(1):1–12
7. Huber S, Butz L, Stegen B, Klumpp D, Braun N, et al. 2013. Ionizing radiation, ion transports, and radioresistance of cancer cells. *Front. Physiol.* 4:212
8. Stark G. 2005. Functional consequences of oxidative membrane damage. *J. Membr. Biol.* 205(1):1–16
9. Cucinotta FA, Durante M. 2006. Cancer risk from exposure to galactic cosmic rays: implications for space exploration by human beings. *Lancet Oncol.* 7(5):431–35
10. Kuncic Z, Lacombe S. 2018. Nanoparticle radio-enhancement: principles, progress and application to cancer treatment. *Phys. Med. Biol.* 63(2):02TR01
11. Kamada T, Tsujii H, Blakely EA, Debus J, De Neve W, et al. 2015. Carbon ion radiotherapy in Japan: an assessment of 20 years of clinical experience. *Lancet Oncol.* 16(2):e93–100
12. Lacombe S, Porcel E, Scifoni E. 2017. Particle therapy and nanomedicine: state of art and research perspectives. *Cancer Nanotechnol.* 8(1):9
13. Lorat Y, Brunner CU, Schanz S, Jakob B, Taucher-Scholz G, Rübe CE. 2015. Nanoscale analysis of clustered DNA damage after high-LET irradiation by quantitative electron microscopy—the heavy burden to repair. *DNA Repair* 28:93–106
14. Sage E, Shikazono N. 2017. Radiation-induced clustered DNA lesions: repair and mutagenesis. *Oxidative DNA Damage Repair* 107:125–35
15. Mavragani IV, Nikitaki Z, Souli MP, Aziz A, Nowsheen S, et al. 2017. Complex DNA damage: a route to radiation-induced genomic instability and carcinogenesis. *Cancers* 9(7):91
16. Kakarougkas A, Jeggo PA. 2014. DNA DSB repair pathway choice: an orchestrated handover mechanism. *Br. J. Radiol.* 87(1035):20130685
17. Asaithamby A, Hu B, Chen DJ. 2011. Unrepaired clustered DNA lesions induce chromosome breakage in human cells. *PNAS* 108(20):8293–98
18. Lukas J, Lukas C, Bartek J. 2011. More than just a focus: the chromatin response to DNA damage and its role in genome integrity maintenance. *Nat. Cell Biol.* 13(10):1161–69
19. Wilson MD, Benlekbir S, Fradet-Turcotte A, Sherker A, Julien J-P, et al. 2016. The structural basis of modified nucleosome recognition by 53BP1. *Nature* 536:100–3
20. Boudaïffa B, Cloutier P, Hunting D, Huels MA, Sanche L. 2000. Resonant formation of DNA strand breaks by low-energy (3 to 20 eV) electrons. *Science* 287(5458):1658–60
21. Alizadeh E, Orlando TM, Sanche L. 2015. Biomolecular damage induced by ionizing radiation: the direct and indirect effects of low-energy electrons on DNA. *Annu. Rev. Phys. Chem.* 66:379–98
22. Dong Y, Gao Y, Liu W, Gao T, Zheng Y, Sanche L. 2019. Clustered DNA damage induced by 2–20 eV electrons and transient anions: general mechanism and correlation to cell death. *J. Phys. Chem. Lett.* 10(11):2985–90
23. Ma J, Wang F, Denisov SA, Adhikary A, Mostafavi M. 2017. Reactivity of prehydrated electrons toward nucleobases and nucleotides in aqueous solution. *Sci. Adv.* 3(12):e1701669
24. Ma J, Kumar A, Muroya Y, Yamashita S, Sakurai T, et al. 2019. Observation of dissociative quasi-free electron attachment to nucleoside via excited anion radical in solution. *Nat. Commun.* 10(1):102
25. Arumainayagam CR, Garrod RT, Boyer MC, Hay AK, Bao ST, et al. 2019. Extraterrestrial prebiotic molecules: photochemistry versus radiation chemistry of interstellar ices. *Chem. Soc. Rev.* 48(8):2293–314
26. Bennett CJ, Pirim C, Orlando TM. 2013. Space-weathering of solar system bodies: a laboratory perspective. *Chem. Rev.* 113(12):9086–150
27. Nass K. 2019. Radiation damage in protein crystallography at X-ray free-electron lasers. *Acta Crystallogr. Sect. D* 75(2):211–18
28. Bury C, Garman EF, Ginn HM, Ravelli RBG, Carmichael I, et al. 2015. Radiation damage to nucleoprotein complexes in macromolecular crystallography. *J. Synchrotron Radiat.* 22:213–24
29. Loh Z-H, Doumy G, Arnold C, Kjellsson L, Southworth SH, et al. 2020. Observation of the fastest chemical processes in the radiolysis of water. *Science* 367(6474):179

30. Trinter F, Schöffler MS, Kim H-K, Sturm FP, Cole K, et al. 2014. Resonant Auger decay driving intermolecular Coulombic decay in molecular dimers. *Nature* 505(7485):664–66
31. Calegari F, Ayuso D, Trabattoni A, Belshaw L, De Camillis S, et al. 2014. Ultrafast electron dynamics in phenylalanine initiated by attosecond pulses. *Science* 346(6207):336
32. Belloni J, Monard H, Gobert F, Larbre J-P, Demarque A, et al. 2005. ELYSE—a picosecond electron accelerator for pulse radiolysis research. *Nucl. Instrum. Methods Phys. Res. Sect. A* 539(3):527–39
33. Thürmer S, Ončák M, Ottosson N, Seidel R, Hergenhahn U, et al. 2013. On the nature and origin of dicationic, charge-separated species formed in liquid water on X-ray irradiation. *Nat. Chem.* 5(7):590–96
34. Dinh PM, du Bourg LB, Gao C-Z, Gu B, Lacombe L, et al. 2017. On the quantum description of irradiation dynamics in systems of biological relevance. In *Nanoscale Insights into Ion-Beam Cancer Therapy*, ed. AV Solov'yov, pp. 277–309. Cham, Switz.: Springer Int.
35. Kohanoff J, McAllister M, Tribello GA, Gu B. 2017. Interactions between low energy electrons and DNA: a perspective from first-principles simulations. *J. Phys. Condens. Matter* 29(38):383001
36. Gu J, Leszczynski J, Schaefer HF. 2012. Interactions of electrons with bare and hydrated biomolecules: from nucleic acid bases to DNA segments. *Chem. Rev.* 112(11):5603–40
37. Monari A, Dumont E. 2015. Understanding DNA under oxidative stress and sensitization: the role of molecular modeling. *Front. Chem.* 3:43
38. Tavernelli I. 2015. Nonadiabatic molecular dynamics simulations: synergies between theory and experiments. *Acc. Chem. Res.* 48(3):792–800
39. Parise A, Alvarez-Ibarra A, Wu X, Zhao X, Pilmé J, de la Lande A. 2018. Quantum chemical topology of the electron localization function in the field of attosecond electron dynamics. *J. Phys. Chem. Lett.* 9(4):844–50
40. Howell RW. 2008. Auger processes in the 21st century. *Int. J. Radiat. Biol.* 84(12):959–75
41. Cederbaum LS, Zobeley J, Tarantelli F. 1997. Giant intermolecular decay and fragmentation of clusters. *Phys. Rev. Lett.* 79(24):4778–81
42. von Sonntag C. 2010. Radiation-induced DNA damage: indirect effects. In *Recent Trends in Radiation Chemistry*, ed. JF Wishart, pp. 543–62. London: World Scientific
43. Becker D, Adhikary A, Sevilla MD. 2010. Mechanisms of radiation-induced DNA damage: direct effects. In *Recent Trends in Radiation Chemistry*, ed. JF Wishart, pp. 509–42. London: World Scientific
44. LaVere T, Becker D, Sevilla MD. 1996. Yields of $OH^{\cdot}$ in gamma-irradiated DNA as a function of DNA hydration: hole transfer in competition $OH^{\cdot}$ formation. *Radiat Res.* 145:673
45. Cederbaum LS, Zobeley J. 1999. Ultrafast charge migration by electron correlation. *Chem. Phys. Lett.* 307(3):205–10
46. Friedland W, Dingfelder M, Kundrát P, Jacob P. 2011. Track structures, DNA targets and radiation effects in the biophysical Monte Carlo simulation code PARTRAC. *Mutat. Res.* 711(1–2):28–40
47. Francis Z, Incerti S, Karamitros M, Tran HN, Villagrasa C. 2011. Stopping power and ranges of electrons, protons and alpha particles in liquid water using the Geant4-DNA package. *Nucl. Instrum. Methods Phys. Res. Sect. B* 269(20):2307–11
48. Marante C, Klinker M, Corral I, González-Vázquez J, Argenti L, Martín F. 2017. Hybrid-basis close-coupling interface to quantum chemistry packages for the treatment of ionization problems. *J. Chem. Theory Comput.* 13(2):499–514
49. Jagau T-C, Bravaya KB, Krylov AI. 2017. Extending quantum chemistry of bound states to electronic resonances. *Annu. Rev. Phys. Chem.* 68:525–53
50. Miteva T, Kazandjian S, Sisourat N. 2017. On the computations of decay widths of Fano resonances. *Chem. Phys.* 482:208–15
51. Whitenack DL, Wasserman A. 2011. Density functional resonance theory of unbound electronic systems. *Phys. Rev. Lett.* 107(16):163002
52. Runge E, Gross EKU. 1984. Density-functional theory for time-dependent systems. *Phys. Rev. Lett.* 52(12):997–1000
53. Calvayrac F, Reinhard PG, Suraud E. 1995. Nonlinear plasmon response in highly excited metallic clusters. *Phys. Rev. B.* 52(24):R17056–59
54. Yabana K, Bertsch GF. 1996. Time-dependent local-density approximation in real time. *Phys. Rev. B.* 54(7):4484–87

55. Flick J, Ruggenthaler M, Appel H, Rubio A. 2015. Kohn-Sham approach to quantum electrodynamical density-functional theory: exact time-dependent effective potentials in real space. *PNAS* 112(50):15285
56. Wu X, Alvarez-Ibarra A, Salahub DR, de la Lande A. 2018. Retardation in electron dynamics simulations based on time-dependent density functional theory. *Eur. Phys. J. D* 72(12):206
57. Rizzi V, Todorov TN, Kohanoff JJ. 2017. Inelastic electron injection in a water chain. *Sci. Rep.* 7(1):45410
58. Schild A, Gross EKU. 2017. Exact single-electron approach to the dynamics of molecules in strong laser fields. *Phys. Rev. Lett.* 118(16):163202
59. Zhao L, Tao Z, Pavošević F, Wildman A, Hammes-Schiffer S, Li X. 2020. Real-time time-dependent nuclear–electronic orbital approach: dynamics beyond the Born–Oppenheimer approximation. *J. Phys. Chem. Lett.* 11(10):4052–58
60. Castro A, Marques MAL, Rubio A. 2004. Propagators for the time-dependent Kohn-Sham equations. *J. Chem. Phys.* 121(8):3425–33
61. Gómez Pueyo A, Marques MAL, Rubio A, Castro A. 2018. Propagators for the time-dependent Kohn-Sham equations: multistep, Runge-Kutta, exponential Runge-Kutta, and commutator free Magnus methods. *J. Chem. Theory Comput.* 14(6):3040–52
62. Schleife A, Draeger EW, Anisimov VM, Correa AA, Kanai Y. 2014. Quantum dynamics simulation of electrons in materials on high-performance computers. *Comput. Sci. Eng.* 16(5):54–60
63. Andrade X, Strubbe D, De Giovannini U, Larsen AH, Oliveira MJT, et al. 2015. Real-space grids and the Octopus code as tools for the development of new simulation approaches for electronic systems. *Phys. Chem. Chem. Phys.* 17(47):31371–96
64. Kühne TD, Iannuzzi M, Del Ben M, Rybkin VV, Seewald P, et al. 2020. CP2K: an electronic structure and molecular dynamics software package – Quickstep: efficient and accurate electronic structure calculations. *J. Chem. Phys.* 152(19):194103
65. Köster AM, Reveles JU, del Campo JM. 2004. Calculation of exchange-correlation potentials with auxiliary function densities. *J. Chem. Phys.* 121(8):3417–24
66. Dunlap BI, Rösch N, Trickey SB. 2010. Variational fitting methods for electronic structure calculations. *Mol. Phys.* 108(21–23):3167–80
67. The 26emon dev. 2019. deMon2k: a software package for density functional theory (DFT) calculations. *deMon2k*. **http://www.demon-software.com/public_html/index.html**
68. Mejía-Rodríguez D, Köster AM. 2014. Robust and efficient variational fitting of Fock exchange. *J. Chem. Phys.* 141(12):124114
69. Delesma FA, Geudtner G, Mejía-Rodríguez D, Calaminici P, Köster AM. 2018. Range-separated hybrid functionals with variational fitted exact exchange. *J. Chem. Theory Comput.* 14(11):5608–16
70. de la Lande A, Clavaguéra C, Köster A. 2017. On the accuracy of population analyses based on fitted densities. *J. Mol. Model.* 23(4):99
71. Choi J, Demmel J, Dhillon I, Dongarra J, Ostrouchov S, et al. 1996. ScaLAPACK: a portable linear algebra library for distributed memory computers—design issues and performance. *Comp. Phys. Comm.* 97(1–2):1–15
72. de la Lande A, Alvarez-Ibarra A, Hasnaoui K, Cailliez F, Wu X, et al. 2019. Molecular simulations with in-deMon2k QM/MM, a tutorial-review. *Molecules* 24(9):1653
73. Wu X, Teuler J-M, Cailliez F, Clavaguéra C, Salahub DR, de la Lande A. 2017. Simulating electron dynamics in polarizable environments. *J. Chem. Theory Comput.* 13(9):3985–4002
74. Li X, Tully JC, Schlegel HB, Frisch MJ. 2005. *Ab initio* Ehrenfest dynamics. *J. Chem. Phys.* 123(8):084106
75. Tavernelli I, Röhrig UF, Rothlisberger U. 2005. Molecular dynamics in electronically excited states using time-dependent density functional theory. *Mol. Phys.* 103(6–8):963–81
76. Schleife A, Kanai Y, Correa AA. 2015. Accurate atomistic first-principles calculations of electronic stopping. *Phys. Rev. B* 91(1):014306
77. IAEA (Int. At. Energy Agency). 2020. *Electronic Stopping Power of Matter for Ions*. Nucl. Data Serv.: Graphs, Data, Comments and Programs, Vienna, Austria, updated Feb. 20. **https://www-nds.iaea.org/stopping/**
78. Ziegler JF. 2016. SRIM - The Stopping and Range of Ions in Matter. *Interactions of Ions with Matter*. **http://srim.org**

79. Mozumder A, Hatano Y. 2004. *Charged Particle and Photon Interactions with Matter*. New York: Marcel Dekker
80. Shukri AA, Bruneval F, Reining L. 2016. *Ab initio* electronic stopping power of protons in bulk materials. *Phys. Rev. B* 93(3):035128
81. Maliyov I, Crocombette J-P, Bruneval F. 2020. Quantitative electronic stopping power from localized basis set. *Phys. Rev. B* 101(3):035136
82. Correa AA. 2018. Calculating electronic stopping power in materials from first principles. *Comput. Mater. Sci.* 150:291–303
83. Yost DC, Yao Y, Kanai Y. 2017. Examining real-time time-dependent density functional theory nonequilibrium simulations for the calculation of electronic stopping power. *Phys. Rev. B* 96(11):115134
84. Yu HS, Li SL, Truhlar DG. 2016. Perspective: Kohn-Sham density functional theory descending a staircase. *J. Chem. Phys.* 145(13):130901
85. Fuks JI, Lacombe L, Nielsen SEB, Maitra NT. 2018. Exploring non-adiabatic approximations to the exchange-correlation functional of TDDFT. *Phys. Chem. Chem. Phys.* 20(41):26145–60
86. Ullrich CA, Yang Z. 2014. A brief compendium of time-dependent density functional theory. *Braz. J. Phys.* 44(1):154–88
87. Dinh PM, Lacombe L, Reinhard P-G, Suraud É, Vincendon M. 2018. On the inclusion of dissipation on top of mean-field approaches. *Eur. Phys. J. B* 91(10):246
88. Privett AJ, Teixeira ES, Stopera C, Morales JA. 2017. Exploring water radiolysis in proton cancer therapy: time-dependent, non-adiabatic simulations of $H^+ + (H_2O)_{1–6}$. *PLOS ONE* 12(4):e0174456
89. Reeves KG, Kanai Y. 2017. Electronic excitation dynamics in liquid water under proton irradiation. *Sci. Rep.* 7(1):40379
90. Yost DC, Kanai Y. 2019. Electronic excitation dynamics in DNA under proton and α-particle irradiation. *J. Am. Chem. Soc.* 141(13):5241–51
91. Alvarez-Ibarra A, Parise A, Hasnaoui K, de la Lande A. 2020. The physical stage of radiolysis of solvated DNA by high-energy-transfer particles: insights from new first principles simulations. *Phys. Chem. Chem. Phys.* 22(15):7747–58
92. Trabattoni A, Galli M, Lara-Astiaso M, Palacios A, Greenwood J, et al. 2019. Charge migration in photoionized aromatic amino acids. *Philos. Trans. R. Soc. A* 377(2145):20170472
93. Lara-Astiaso M, Galli M, Trabattoni A, Palacios A, Ayuso D, et al. 2018. Attosecond pump-probe spectroscopy of charge dynamics in tryptophan. *J. Phys. Chem. Lett.* 9(16):4570–77
94. Rozzi CA, Falke SM, Spallanzani N, Rubio A, Molinari E, et al. 2013. Quantum coherence controls the charge separation in a prototypical artificial light-harvesting system. *Nat. Commun.* 4:1602
95. Vacher M, Bearpark MJ, Robb MA, Malhado JP. 2017. Electron dynamics upon ionization of polyatomic molecules: coupling to quantum nuclear motion and decoherence. *Phys. Rev. Lett.* 118(8):083001
96. Polyak I, Jenkins AJ, Vacher M, Bouduban MEF, Bearpark MJ, Robb MA. 2018. Charge migration engineered by localisation: electron-nuclear dynamics in polyenes and glycine. *Mol. Phys.* 116(19–20):2474–89
97. Nijjar P, Jankowska J, Prezhdo OV. 2019. Ehrenfest and classical path dynamics with decoherence and detailed balance. *J. Chem. Phys.* 150(20):204124
98. Min SK, Agostini F, Tavernelli I, Gross EKU. 2017. Ab initio nonadiabatic dynamics with coupled trajectories: a rigorous approach to quantum (de)coherence. *J. Phys. Chem. Lett.* 8(13):3048–55
99. Cai Z, Chen S, Wang L-W. 2019. Dissociation path competition of radiolysis ionization-induced molecule damage under electron beam illumination. *Chem. Sci.* 10(46):10706–15
100. Geerlings P, Chamorro E, Chattaraj PK, De Proft F, Gázquez JL, et al. 2020. Conceptual density functional theory: status, prospects, issues. *Theor. Chem. Acc.* 139(2):36
101. Chauvin R, Lepetit C, Silvi B, Alikhani E, ed. 2016. *Challenges and Advances in Computational Chemistry and Physics*, Vol. 22: *Applications of Topological Methods in Molecular Chemistry*. Cham, Switz.: Springer Int.
102. Pilmé J, Luppi E, Bergès J, Houée-Lévin C, de la Lande A. 2014. Topological analyses of time-dependent electronic structures: application to electron-transfers in methionine enkephalin. *J. Mol. Model.* 20(8):2368
103. Burnus T, Marques MAL, Gross EKU. 2005. Time-dependent electron localization function. *Phys. Rev. A* 71(1):010501

104. Schnitker J, Rossky PJ. 1987. Quantum simulation study of the hydrated electron. *J. Chem. Phys.* 86(6):3471–85
105. Nicolas C, Boutin A, Lévy B, Borgis D. 2003. Molecular simulation of a hydrated electron at different thermodynamic state points. *J. Chem. Phys.* 118(21):9689–96
106. Savolainen J, Uhlig F, Ahmed S, Hamm P, Jungwirth P. 2014. Direct observation of the collapse of the delocalized excess electron in water. *Nat. Chem.* 6(8):697–701
107. Li X, Sevilla MD, Sanche L. 2003. Density functional theory studies of electron interaction with DNA: can zero eV electrons induce strand breaks? *J. Am. Chem. Soc.* 125(45):13668–69
108. Schyman P, Laaksonen A. 2008. On the effect of low-energy electron induced DNA strand break in aqueous solution: a theoretical study indicating guanine as a weak link in DNA. *J. Am. Chem. Soc.* 130(37):12254–55
109. Chen H-Y, Yang P-Y, Chen H-F, Kao C-L, Liao L-W. 2014. DFT reinvestigation of DNA strand breaks induced by electron attachment. *J. Phys. Chem. B* 118(38):11137–44
110. Li X, Sanche L, Sevilla MD. 2006. Base release in nucleosides induced by low-energy electrons: a DFT study. *Radiat. Res.* 165(6):721–29
111. Kumar A, Becker D, Adhikary A, Sevilla MD. 2019. Reaction of electrons with DNA: radiation damage to radiosensitization. *Int. J. Mol. Sci.* 20(16):3998
112. Smyth M, Kohanoff J. 2011. Excess electron localization in solvated DNA bases. *Phys. Rev. Lett.* 106(23):238108
113. McAllister M, Smyth M, Gu B, Tribello GA, Kohanoff J. 2015. Understanding the interaction between low-energy electrons and DNA nucleotides in aqueous solution. *J. Phys. Chem. Lett.* 6(15):3091–97
114. Gu B, Smyth M, Kohanoff J. 2014. Protection of DNA against low-energy electrons by amino acids: a first-principles molecular dynamics study. *Phys. Chem. Chem. Phys.* 16(44):24350–58
115. Marsalek O, Elles CG, Pieniazek PA, Pluhařová E, VandeVondele J, et al. 2011. Chasing charge localization and chemical reactivity following photoionization in liquid water. *J. Chem. Phys.* 135(22):224510
116. Wang F, Schmidhammer U, de La Lande A, Mostafavi M. 2017. Ultra-fast charge migration competes with proton transfer in the early chemistry of $H_2O^{\cdot+}$. *Phys. Chem. Chem. Phys.* 19(4):2894–99
117. López-Tarifa P, Gaigeot M-P, Vuilleumier R, Tavernelli I, Alcamí M, et al. 2013. Ultrafast damage following radiation-induced oxidation of uracil in aqueous solution. *Angew. Chem. Int. Ed.* 52(11):3160–63
118. López-Tarifa P, du Penhoat M-AH, Vuilleumier R, Gaigeot M-P, Tavernelli I, et al. 2012. Ultrafast non-adiabatic fragmentation dynamics of doubly charged uracil in gas and liquid phase. *J. Phys. Conf. Ser.* 388(10):102055
119. López-Tarifa P, du Penhoat M-AH, Vuilleumier R, Gaigeot M-P, Tavernelli I, et al. 2011. Ultrafast nonadiabatic fragmentation dynamics of doubly charged uracil in a gas phase. *Phys. Rev. Lett.* 107(2):023202
120. du Penhoat M-AH, Moraga NR, Gaigeot M-P, Vuilleumier R, Tavernelli I, Politis M-F. 2018. Proton collision on deoxyribose originating from doubly ionized water molecule dissociation. *J. Phys. Chem. A* 122(24):5311–20
121. López-Tarifa P, Grzegorz D, Piekarski Rossich E, du Penhoat M-AH, et al. 2014. Ultrafast nonadiabatic fragmentation dynamics of biomolecules. *J. Phys. Conf. Ser.* 488(1):012037